FORMATION OF THE NEUTRON DONOR ^{13}C IN AGB STARS BY OVERSHOOT AND ROTATION

FALK HERWIG[1] AND NORBERT LANGER[2]

[1] *Universität Potsdam, Potsdam, Germany (fherwig@astro.physik.uni-potsdam.de)*
[2] *Universitet Utrecht, Utrecht, The Netherlands (N.Langer@astro.uu.nl)*

ABSTRACT. Observations of heavy elements in Red Giant stars clearly show that low-mass AGB stars can provide a nucleosynthesis site of the *s*-process. Stellar evolution models produced over the last years indicate that radiative burning of ^{13}C between succeeding thermal pulses in low-mass AGB star models may indeed provide the neutrons for the *s*-process. However, although it seems clear that some mixing between the proton-rich envelope and the carbon-rich core may lead to the production of ^{13}C, the physical mechanism responsible for such mixing is not yet unambiguously identified.

We present stellar model calculations which include mixing due to *overshoot* and *rotation*. Overshoot, with a time-dependent and exponentially decaying efficiency, leads to a partial mixture of protons and ^{12}C during the third dredge-up, when the envelope convection zone reaches deep into the core. According to the depth-dependent ratio of protons and ^{12}C, a small ^{13}C pocket forms underneath a ^{14}N-rich layer. Overshoot does not allow for any mixing after the envelope convection zone retreats at the end of the third dredge-up after each pulse.

Rotation introduces mixing driven by large angular velocity gradients which form at the envelope-core interface in AGB stars, in particular after a thermal pulse. This leads to partial mixing after a pulse, as in the case of overshoot. However, both mechanisms differ during the interpulse phase. Rotation continues to mix the region of the ^{13}C-pocket with a diffusion coefficient of $logD \sim 2 \ldots 3 \mathrm{cm}^2\mathrm{s}^{-1}$. This does not only spread the ^{13}C-pocket, but also the more massive ^{14}N-rich layer, and finally leads to mixture of both layers. By the time when the temperature there has risen to about $9\,10^7$ K and neutron production sets in, the ^{14}N abundance exceeds the ^{13}C abundance by a factor of $5 \ldots 10$. We analyze the role of ^{14}N as a neutron poison by considering the recycling of neutrons via $^{14}\mathrm{N}(\mathrm{n},\mathrm{p})^{14}\mathrm{C}$ and $^{12}\mathrm{C}(p,\gamma)^{13}\mathrm{N}(\beta^+)^{13}\mathrm{C}$ qualitatively. We find that as long as $X(^{14}\mathrm{N}) \ll X(^{12}\mathrm{C})$, the *s*-process will still be possible to occur under radiative conditions.

1. Introduction

Observationally, AGB stars show a clear signature of ongoing *s*-process-nucleosynthesis. Among the evidence is the detection of the radioactively unstable element Tc (Merill 1952). Its longest living isotope, ^{99}Tc, has a half-life of $2.1 \cdot 10^5$yr which clearly exceeds the life time of a thermally pulsing AGB star. Thus, any detected Tc must have been produced *in situ*. More evidence comes, e.g., from the correlation of heavy element abundances (like the index [hs/ls]) with metallicity (Busso et al. 1999) or with the fluorine abundance (Jorissen et al. 1992). Another source of information are pre-solar dust grains from meteorites. Most of the silicon carbide and corundum grains formed in the winds of red giants and AGB stars (Hoppe & Zinner, 2000). The grains allow a determination of the thermodynamic conditions of the *s*-process via precise measurements of the

branching ratios of, e.g., krypton, which supports AGB stars as *s*-process-site.

The current scenario of the *s*-process in AGB stars is closely connected to the alternating mixing and nuclear burning events which characterize the thermal pulse cycle. For any *s*-process in AGB stars, the third dredge-up is a necessary ingredient. It leads to a contact layer where the H-rich envelope and the carbon-rich intershell region can exchange some material and form a partially mixed zone. Gallino et al. (1998) have assumed that a proton-enriched layer forms at the bottom of the convective envelope at the end of the third dredge-up phase. In the further course of the TP cycle, this carbon-rich layer allows the formation of excess ^{13}C. Due to the assumed low proton abundance, no ^{14}N was produced and therefore the role of this isotope as a neutron poison could be neglected. This so-called ^{13}C-pocket is the indispensable prerequisite for the radiative neutron-capture nucleosynthesis during the interpulse phase in AGB stars (Straniero et al. 1995, Gallino et al. 1998). This paper presents two physical candidate processes for the formation of such a ^{13}C-pocket at the envelope-core interface of low-mass AGB stars: rotation and overshoot.

In Sect. 2 we review the properties of the overshoot mechanism as originally proposed for AGB stars by Herwig et al. (1997). Following Sect. 3 gives updated account of AGB models with rotation. A comparison and discussion is presented in Sect. 4

2. Overshoot models

The relevance of overshoot in AGB stars for the neutron source problem has been studied by Herwig et al. (1997, 1999). We assumed that the depth dependence of the mixing due to convective overshoot can be described by an exponentially decaying efficiency. This behavior is qualitatively suggested by many hydrodynamical simulations of convection under various conditions. Freytag et al. (1996) found that the particle spread due to successive convective downdrafts and plumes which reach beyond the convective boundary can be described by a diffusion-like process. Moreover, the velocity field in the stable region declines exponentially. Accordingly the material mixing in the overshoot region can be approximated by a diffusion coefficient which decreases exponentially from a MLT value inside the convective boundary. Herwig (2000) presents the evolution of the abundance profiles of the core-envelope interface during an interpulse period and shows snapshots (Fig. 4) after the ingestion of protons into the intershell layer, after the initial proton capture phase where the ^{13}C-pocket is formed and after consumption of ^{13}C due to α-capture. The situation is sketched in Fig. 1. The main difference to the previously and in detail studied profile by Gallino et al. (1998) is the continuous variation of both the proton- and the ^{12}C-abundance and thus the p/^{12}C - ratio. This ratio determines the ^{13}C/^{14}N - ratio after consumption of hydrogen in the respective layer (Fig. A.1 in Herwig 1998). In the overshoot case we found that the partial mixing zone consists of two adjacent regions after the end of proton captures. Further outward a region with ^{14}N as the most abundant element forms. All ^{12}C is transformed into ^{14}N which reaches a mass fraction of $\sim 40\%$ in models where overshoot has been applied to all convective boundaries. Below this zone the actual ^{13}C-pocket forms where the proton abundance is too low to continue p-captures after the production of ^{13}C. Here, ^{14}N is only of very small abundance. Preliminary *s*-process studies of this situation have shown that quali-

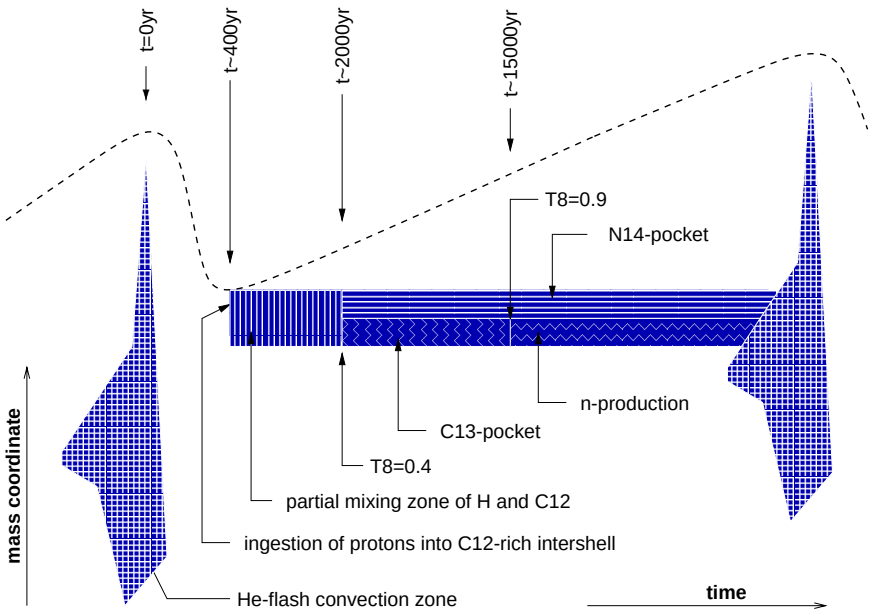

Fig. 1. Schematic representation of the radiative *s*-process during the interpulse phase of TP-AGB stars with a ^{13}C pocket due to overshoot (instantaneous ingestion of protons into the ^{12}C-rich intershell). The two small-checked zones represent the convective He-flash region while the other shaded regions denote the partial mixing zone during different stages: coexistence of protons and ^{12}C (vertically hatched region), ^{14}N-pocket (horizontally hatched), ^{13}C-pocket (vertical zigzag hatch), burning of ^{13}C, n-production (horizontal zigzag hatch). Note, that in the overshoot picture no mixing of the n-production layer is allowed after the retreat of the envelope convection zone.

tatively the reproduction of a solar-like distribution of the main *s*-process-component is possible (Gallino & Herwig, 1998). However, it should be emphasized that the efficiency of overshoot, hence the velocity scale height is a free parameter. Currently we can not constrain the velocity scale height at the bottom of the convective envelope of AGB stars during the dredge-up. For most of the evolutionary phases we used a value of $f = 0.016$ ($H_{\rm v} = f \cdot H_{\rm p}$, $H_{\rm p}$ pressure scale height) which reproduces the width of the main-sequence of intermediate mass stars. However, this value produces only a pocket of integrated ^{13}C of $3 \cdot 10^{-7}\,{\rm M}_{\odot}$. This small amount of ^{13}C leads to fairly small enhancement factors. With a larger overshoot efficiency ($f = 0.128$) we found enhancement factors of ~ 100 for the main component.

Another interesting property of the *s*-process in low-mass AGB stars is now emerging from high precision measurements of pre-solar grains (A. Davis, this volume). Apparently these new observational data require for a model sequence of given initial mass and metalicity a spread in neutron exposures in the range up to a factor of up to 10. Such a spread can not currently be reproduced by the overshoot scenario (however, see Lugaro & Herwig, in prep.). Although the absolute amount of ^{13}C is likely to be

dependent on mass and metallicity for a given velocity scale height of the overshoot, we can not assume that stars even of different mass and metallicities have so greatly different overshoot efficiencies at this convective boundary as to account for the spread required by the pre-solar dust grains. It does seem possible that the overshoot decay has a different rate at different convective boundaries and during different evolutionary phases. Freytag et al. (1996) found $f = 0.25 \ldots 1$ for the shallow surface convection zones of A-stars and white dwarfs. Such a large value is certainly not appropriate in the adiabatic core regions and can in fact be excluded for the main-sequence convective core of intermediate mass stars. However, within the physical picture of overshoot the efficiency of this mechanism should be of the same order within a small range in similar evolutionary conditions.

3. Rotation models

Rotationally induced mixing is another physical process which might be responsible for the formation of the neutron donor ^{13}C at the envelope-core interface of low-mass AGB stars. In particular, it may introduce a statistical signature on the *s*-process of otherwise identical stars due to a spread of initial rotational velocities. Here we present more detailed properties of the AGB models by Langer et al. (1999) with respect to the formation and destruction of ^{13}C.

3.1. Input physics and stellar models

The input physics is the same as in Heger et al. (2000). The 1D-hydrodynamic stellar evolution code contains angular momentum as an additional state variable, and the effect of centrifugal force on stellar structure. Rotationally induced transport of angular momentum and chemical species are taken into account according to Eddington-Sweet circulations, the Solberg-Hoiland and the Goldreich-Schubert-Fricke instability, as well as dynamical and secular shear instabilities. The μ-gradient acts as barrier for rotationally induced mixing ($f_\mu = 0.05$) and convection (Ledoux-criterion, semi-convection). Nucleosynthesis is treated by a network with pp-chain, CNO-, NeNa- and MgAl-cycles, He-burning including (α, n) reactions and the inclusion of (n, γ) reactions. Here we also discuss the additional effect of the $^{14}\mathrm{N(n,p)}^{14}\mathrm{C}$ reaction.

The stellar model sequence had an initial mass of $3\,\mathrm{M}_\odot$ and initial equatorial rotation velocity of 250km/s and was evolved to the AGB with mass loss. Contrary to the models with overshoot dredge-up sets in fairly late and remains week. The TP cycle described below is the 25^{th} ($\mathrm{M_c} = 0.746\,\mathrm{M}_\odot$) and the dredge-up just reaches into the carbon-rich intershell. Sufficient carbon star formation can not be expected from these models.

3.2. Rotationally induced mixing, formation and evolution of the ^{13}C-pocket

In a very generalized sense rotationally induced mixing occurs where large angular velocity gradients develop. In addition, convective transport of angular momentum enforces close-to-ridged rotation. Conservation of angular momentum leads to a decrease (increase) of angular velocity in expanding (contracting) layers. These mechanisms can be seen at work during a thermal pulse and the subsequent interpulse phase in Fig. 2. At

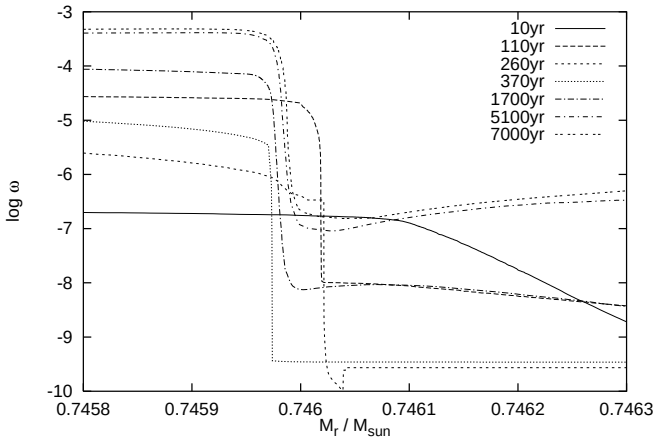

Fig. 2. Evolution of angular velocity during the $25^{\rm th}$ thermal pulse and the following first third of the interpulse phase in the stellar interface region of envelope and core (cf. Fig. 3 in Langer et al. 1999). The left part of the diagram below the mass coordinate $\sim 0.746\,{\rm M}_\odot$ corresponds to the top of the intershell region, the right part shows the bottom of the envelope. The time 10yr corresponds to the onset of the He-flash just before the luminosity peak is reached.

the onset of the He-flash (10yr) the pulse-driven convection zone is developing but has not yet reached the interface region shown in Fig. 2. Accordingly the angular velocity profile runs still smoothly in the interface region. At (110yr) - shortly after the maximum extension of the He-flash convection zone into the interface layer - convection has lifted the angular velocity below the interface and left behind a prominent step-like edge. At the same time the descending envelope convection bottom decreases the angular velocity above the interface which leads to an even larger angular velocity gradient. About 150yr later the angular velocity in the upper core region decreases due to the expansion of that layer following the energy ingestion further below during the thermo-nuclear runaway of the He-shell. However, during this phase the maximum angular velocity gradient is reached and the velocity difference in the top layer of the core and the bottom layer of the envelope amounts to about five orders of magnitude.

During the further interpulse evolution the angular velocity generally increases because contraction resumes in between the thermal pulses. The angular velocity step, however, decreases only slowly. At 7000yr – half way from ^{13}C-formation to -destruction – the angular velocity step at the interface still comprises almost four orders of magnitude. Thus, rotationally induced mixing at the interface of core and envelope after a thermal pulse and during the interpulse is *ongoing*. This is an important difference to the overshoot picture where no mixing occurs during the interpulse phase in the interface layer and the interpulse nucleosynthesis is *static*.

Although the physical principles of mixing in the overshoot and the rotational case are very different the abundance profiles at the time after the initial proton-capture

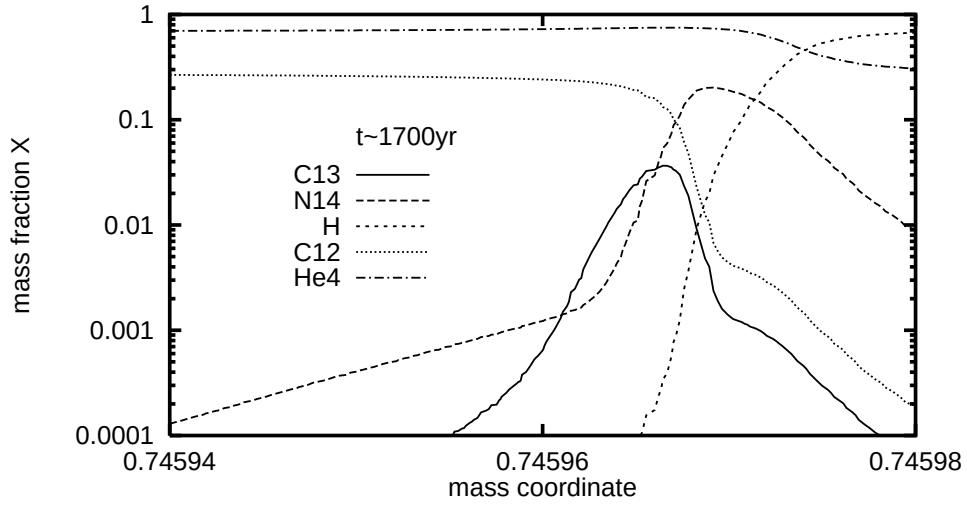

Fig. 3. Abundance profiles when the ^{13}C pocket has formed at the interface of core and envelope from the partial mixing of protons and ^{12}C due to rotationally induced mixing.

phase in the partial mixing zone are quite similar. The case where partial mixing is caused by rotation is displayed in Fig. 3. Clearly visible are two neighboring zones where ^{13}C and ^{14}N respectively are dominating. Another similarity to the overshoot case is the negative curvature of the proton profile in the overshoot region just before the onset of proton captures (a few hundred years before the situation shown in Fig. 3). A difference to the overshoot case is the larger extent of the partial mixing zone and the tail of ^{14}N which reaches deep into the intershell even below the ^{13}C-pocket itself. This ^{14}N tail is due to the fact that the dredge-up is fairly weak and (by coincidence?) just reaches the top of the intershell region which has been homogenized by the previous thermal pulse. A pronounced region of rotationally induced mixing which forms shadow-like in the upper part of the receding He-flash convection zone (cf. Fig. 3 in Langer et al. 1999) causes exchange of material with the ^{14}N-rich He-buffer zone, left over by H-shell burning during the previous intershell phase.

During the following phase the ^{13}C pocket is subject to continuous modification and the evolution is shown in Fig. 4. It takes about $\sim$ 8000yr from the end of ^{13}C-formation (at $\sim$ 1700yr) to the onset of neutron production ($\sim$ 10000yr)[1]. The abundance profile change during this phase shows a broadening and lowering of the peak ^{13}C-abundance and is due only to rotationally induced mixing. Even after the α-capture reactions on ^{13}C have started, mixing remains an important contribution to the abundance profile modification (Fig. 4, $t = 14000$yr).

[1] All timescales given are strongly dependent on core mass, and e.g. considerably longer for lower core masses.

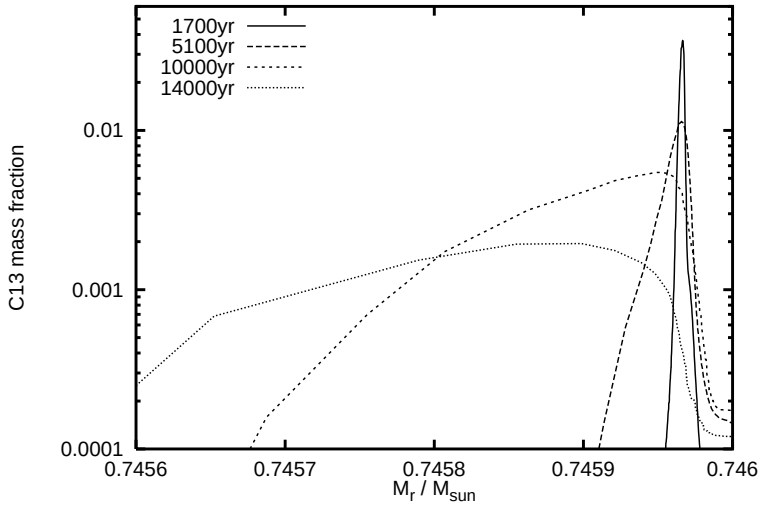

Fig. 4. Evolution of the ^{13}C-pocket after its formation during the first part of the interpulse period. The change of the profile from the initial formation at $\sim$ 1700yr until the onset of α-captures of ^{13}C at about 10000yr is due to rotationally induced mixing. Thereafter, both mixing as well as nuclear burning (neutron production) are responsible for the modification of the abundance profile.

3.3. Recycling of neutrons

The broadening of the ^{13}C-profile and the lowering of the peak ^{13}C-abundance (which reaches 10% in the overshoot case if the extra mixing is applied to all convective boundaries, Herwig 2000) is a feature which at first glance is advantageous for the *s*-process. The neutron density is reduced and the exposure of neutrons is distributed over a larger variety of seed material. However, the role of ^{14}N is of great importance if rotationally induced mixing is efficient. Not only the ^{13}C-pocket is broadening as shown in Fig. 4 but the prominent ^{14}N-pocket shown in Fig. 3 shares this fate. The situation at about the peak neutron production is shown in Fig. 5. The ^{13}C-pocket is entirely wrapped into the broad ^{14}N-pocket. This ^{14}N causes two problems for an efficient *s*-process. The neutron-density is reduced because $^{14}\mathrm{N(n,p)}^{14}\mathrm{C}$ is efficiently *competing* with the n-capture of ^{56}Fe and other heavy elements. Moreover, the released protons from the (n, p) reaction *destroy* ^{13}C and thereby reduce the n-source. ^{14}N adds another efficient n-sink, reduces the available amount of ^{13}C and thereby weakens the n-source.

It is beyond the purpose of this paper to present a full nuclear network analysis of the neutron-recycling initiated by the efficient (n, p) reaction of ^{14}N. However, some qualitative considerations show that the *s*-process is not necessarily prohibited by rotationally induced mixing. Typical conditions during n-production in the interpulse phase are given by $\mathrm{T_8} = 0.9$, $\rho = 3700\mathrm{g/cm^3}$, $X(^{13}\mathrm{C}) = 3 \cdot 10^{-3}$, $X(^{14}\mathrm{N}) = 2 \cdot 10^{-2}$, $X(^{12}\mathrm{C}) = 2 \cdot 10^{-1}$, $X(^{4}\mathrm{He}) = 0.7$ and $X(^{56}\mathrm{Fe}) = 2 \cdot 10^{-3}$ (mass fractions). A rough estimate of the effect

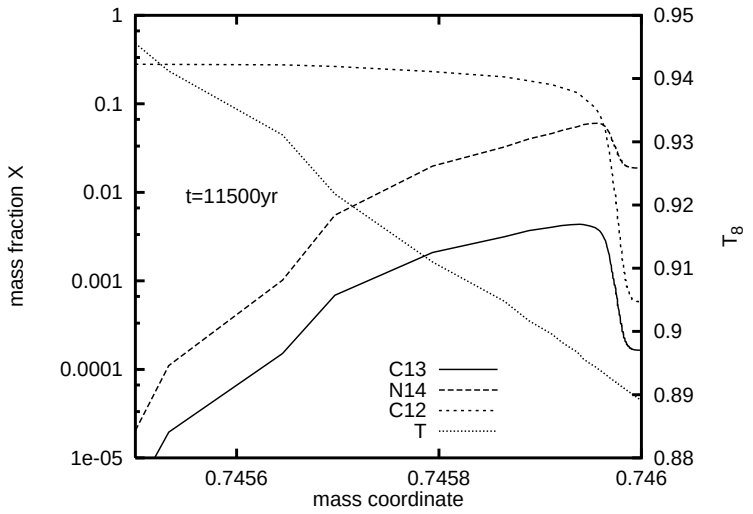

Fig. 5. At $t = 11500$yr the neutron production is close to the maximum. Due to continuous rotationally induced mixing the large ^{14}N-pocket (Fig. 3) has intermingled with the smaller ^{13}C-pocket. Due to this continuous mixing ^{14}N is more abundant than ^{13}C in the region of the pocket. Note, that for the profiles shown here, the (n, p) of ^{14}N has been neglected. The influence of the neutron recycling initiated by this reaction is described in the text.

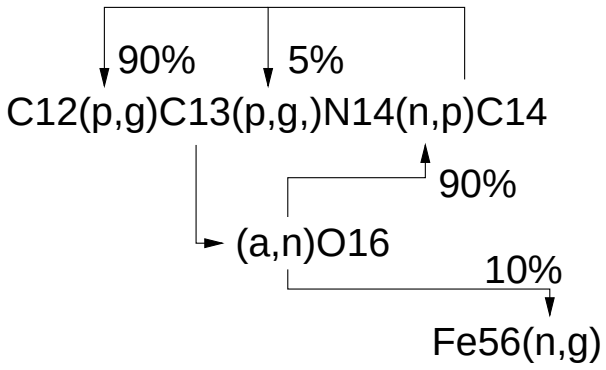

Fig. 6. Schematic representation of the main reactions involved in the recycling of neutrons. The efficient (n, p) reaction of ^{14}N acts as the main competitor for n-captures of the Fe-seeds. If the ^{12}C abundance is large compared to the ^{14}N abundance more neutrons will escape the recycling via Fe-capture than protons via capture by ^{13}C. In that case the *s*-process is possible. The percentages indicate the branching ratios for the particular situation discussed in the text.

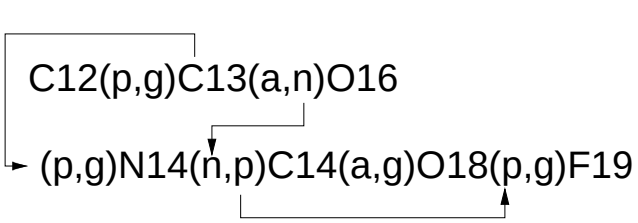

Fig. 7. Possible radiative production of ^{19}F during the interpulse in the partial mixing zone of a rotating AGB star.

of ^{14}N as a neutron sink competing with iron is given by

$$\frac{< \sigma v >_{^{56}\mathrm{Fe,n}} Y_{^{56}\mathrm{Fe}}}{< \sigma v >_{^{14}\mathrm{N},n} Y_{^{14}\mathrm{N}}} \simeq 0.1$$

which ignores other neutron poisons as well as other heavy elements, in particular iron peak elements. Thus, under the given conditions of a partial mixing zone due to rotationally induced mixing, about 9 times more neutrons are captured by ^{14}N than compared to the number captured by ^{56}Fe. The effect of ^{14}N as a source of protons that destroy the neutron source ^{13}C can be estimated by the expression

$$\frac{< \sigma v >_{^{13}\mathrm{C},p} Y_{^{13}\mathrm{C}}}{< \sigma v >_{^{12}\mathrm{C},p} Y_{^{12}\mathrm{C}}} \simeq 0.05$$

where small leakages of protons to $^{18}\mathrm{O}(\mathrm{p},\alpha)^{15}\mathrm{N}$ ($\sim 1\%$) and $^{15}\mathrm{N}(p,\alpha)^{12}\mathrm{C}$ ($\sim 2\%$) are neglected.

The main reactions of the neutron recycling is shown in Fig. 6. The percentages given in the graph represent the ratios derived above. Thus, they are specific to the case discussed here. The chances for the iron seeds to get hold on neutrons are better the higher the ^{12}C abundance and the lower the ^{14}N abundance. The larger the ratio of neutrons captured by ^{56}Fe to protons captured by ^{13}C the higher is the *s*-process efficiency because the relative loss of protons by $^{13}\mathrm{C}(p,\gamma)$ smaller than fraction of neutrons captured by heavy elements. Recycling occurs on timescale of α-capture of ^{13}C ($\sim$ 13000yr at beginning of n-production and decreasing to $\sim$ 1000yr towards end of interpulse phase) and it thus leads to a certain delayed neutron exposure. ^{14}N as a n-poison is less effective compared to the situation in the ^{14}N pocket of an overshoot partial mixing zone because the ^{12}C abundance is larger and the ^{14}N abundance smaller. Finally, the $^{14}\mathrm{N}(n,p)$ reaction releases protons at high temperatures and thus AGB models with rotation may be able to produce at the same time heavy elements and ^{19}F as shown in Fig. 7.

4. Conclusions

In this paper we have discussed in some detail the evolution of the abundance of the neutron donor ^{13}C according to stellar models including overshoot and rotation. Although both processes give promising results, neither of the two classes of models was found to be free of problems and unsolved aspects.

Rotation can produce a ^{13}C-pocket, which, however, is mixed with a ^{14}N-rich layer during the interpulse phase. This makes the consideration of ^{14}N as neutron poison important, although, as shown above, a larger ^{14}N than ^{13}C abundance does not automatically imply that the *s*-process is choked off. In any case, the models with diffusive overshoot are free of this complication as no mixing occurs in the ^{13}C-pocket in between two thermal pulses. This situation has also the advantage that it can be accurately modelled by a series of one-zone nuclear network calculations for the conditions in various layers of the interface region of envelope and core. In order to model the *s*-process in rotating AGB stars, nucleosynthesis calculations in many layers covering the interface region, must be alternated with time-dependent mixing according to the rotationally induced mixing efficiency.

The most important next step will be to quantify the neutron recycling during the interpulse phase in rotating AGB stars. With respect to overshoot, the main problem remains the unknown efficiency of this process. Current models indicate that the *s*-process efficiency reaches acceptable levels within the lifetime of an AGB star only if an overshoot efficiency above that obtained fitting the width of the main sequence band ($f = 0.016$; cf. Herwig et al. 1997, Herwig 1998) is chosen during the dredge-up phase at the bottom of the envelope convection.

At present, we can only conclude that both, rotation and overshoot, have the potential to play an important role in the *s*-process nucleosynthesis in AGB stars, but we are unable to quantify the relative importance of these mechanisms for the production of the neutron donor ^{13}C yet. However, in view of the results presented above, it appears not unlikely that both processes act in fact simultaneously. A study of stellar model sequences including the combined consideration of these two processes will be done in a future investigation.

Acknowledgements

This work has been supported by the *Deutsche Forschungsgemeinschaft, DFG* (La 587/16). We would like to thank Roberto Gallino and Maria Lugaro for important and helpful discussions.

References

Busso, M., Gallino, R., and Wasserburg, G. J., 1999, ARA&A 37, 239
Freytag, B., Ludwig, H.-G., and Steffen, M., 1996, A&A 313, 497
Gallino, R., Arlandini, C., Busso, M., Lugaro, M., Travaglio, C., Straniero, O., Chieffi, A., and Limongi, M., 1998, ApJ 497, 388
Gallino, R. and Herwig, F., 1998, s-process nucleosynthsis in AGB models with overshoot, unpublished
Heger, A., Langer, N., and Woosley, S. E., 2000, ApJ 528, 368
Herwig, F., Blöcker, T., Schönberner, D., and El Eid, M. F., 1997, A&A 324, L81
Herwig, F., 1998, Ph.D. thesis, Universität Kiel, Germany
Herwig, F., Blöcker, T., and Schönberner, D., 1999, in T. L. Bertre, A. Lebre, and C. Waelkens (eds.), AGB Stars, IAU Symp. 191, p. 41

Herwig, F., 2000, A&A, in press, astro-ph/0007139
Hoppe, P. and Zinner, E., 2000, J. Geophys. Res. 105, 10371
Jorissen, A., Smith, V. V., and Lambert, D. L., 1992, A&A 261, 164
Langer, N., Heger, A., Wellstein, S., and Herwig, F., 1999, A&A 346, L37
Merill, P. W., 1952, ApJ 116, 21
Straniero, O., Gallino, R., Busso, M., Chieffi, A., Raiteri, C. M., Salaris, M., and Limongi, M., 1995, ApJ 440, L85